

TOPOLOGICAL OPTICS

Topological phonon-polariton funneling in midinfrared metasurfaces

S. Guddala^{1,2}, F. Komissarenko^{1,2}, S. Kiriushechkina¹, A. Vakulenko¹, M. Li^{1,2,3}, V. M. Menon^{2,3}, A. Alù^{4,3,1}, A. B. Khanikaev^{1,2,3*}

Topological photonics offers enhanced control over electromagnetic fields by providing a platform for robust trapping and guiding of topological states of light. By combining the strong coupling between topological photons with phonons in hexagonal boron nitride (hBN), we demonstrate a platform to control and guide hybrid states of light and lattice vibrations. The observed topological edge states of phonon-polaritons are found to carry nonzero angular momentum locked to their propagation direction, which enables their robust transport. Thus, these topological quasiparticles enable the funneling of infrared phonons mediated by helical infrared photons along arbitrary pathways and across sharp bends, thereby offering opportunities for applications ranging from Raman and vibrational spectroscopy with structured phonon-polaritons to directional heat dissipation.

Topologically nontrivial phases of matter have been affecting our fundamental understanding of the physics of quantum systems. Successfully transferred to the realms of classical physics, topological phases have been realized in a variety of photonic (1, 2), acoustic, and mechanical systems (3, 4). Among classical platforms, topological photonics represents the first example of the successful realization of different topological phases (2). The advantage of classical systems—electromagnetic systems in particular—enabled by their engineering ability, not only facilitates the testing of some of the most peculiar theoretical models of topo-

logical physics but also expands the domain of topological phases into previously unthinkable regimes, such as topological lasers (5–7), non-Hermitian systems (8, 9), and nonlinear topological phases (10–12).

Another advantage of photonic topological systems lies in the ability of electromagnetic fields to interact with a broad range of excitations, from magnons and spin waves to phonons, plasmons, and excitons, which gives rise to the formation of half-light half-matter quasiparticles known as polaritons (13). This opens new realms for topological multiphysics, where topological phases can be transferred from one

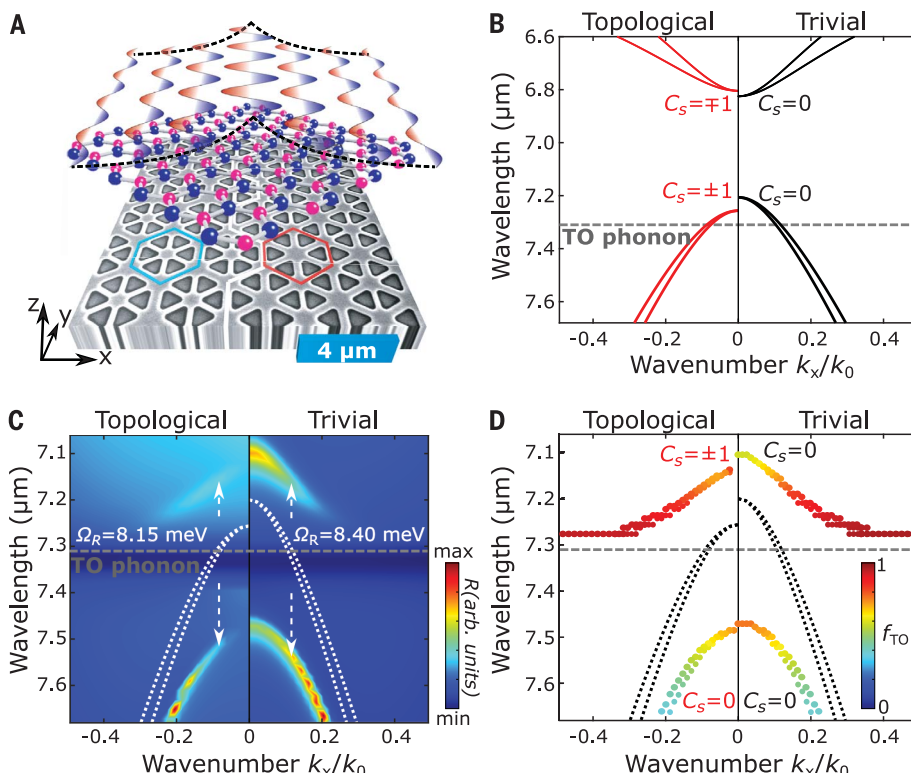
type of physical domain to another or emerge as the result of multiphysics interactions (14–16). Recent work has shown that interactions of light with excitons may lead to the formation of topological exciton-polaritons (17–20).

Here, we demonstrate a topological polaritonic system in which midinfrared (mid-IR) topological photonic states are strongly coupled with in-plane vibrations (phonons) in hBN. Our system consists of a metasurface supporting a spin-Hall-like (Z_2) topological photonic phase (21) with a (few-layer) hBN on top of it (Fig. 1A). The metasurface is formed by an array of triangular holes (22) in silicon-on-sapphire (SOS) substrate. This metasurface geometry is known to undergo a topological transition from a trivial to a nontrivial phase (Fig. 1B) when the design of the unit cell changes from shrunken [triangles within the unit cell are closer to one another than the triangles in the nearby unit cells (Fig. 1A, light blue hexagon)] to expanded [triangles in the unit cell are farther from one another compared with those in the nearby unit cells (Fig. 1A, red hexagon)]. The existence of topological photonic edge states has been extensively studied

¹Department of Electrical Engineering, Grove School of Engineering, City College of the City University of New York, New York, NY 10031, USA. ²Department of Physics, City College of New York, New York, NY 10031, USA. ³Physics Program, Graduate Center of the City University of New York, New York, NY 10016, USA. ⁴Photonics Initiative, Advanced Science Research Center, City University of New York, New York, NY 10031, USA.

*Corresponding author. Email: akhanikaev@ccny.cuny.edu

Fig. 1. Phonon-polaritons in heterostructures formed by a topological mid-IR metasurface loaded by an hBN layer. (A) Schematic of the phonon-polariton system with extruded scanning electron microscopy (SEM) image of the metasurface with a few-layer hBN on top. Light blue and red hexagons indicate unit cells of trivial and topological domains, respectively, and the armchair-shaped white line shows the domain wall. Color waves show transverse phonon oscillations in hBN as a result of topological edge polaritons. (B) Photonic band structure of topological and trivial mid-IR metasurfaces. A dashed line indicates the spectral position of the TO phonon mode in hBN. (C) Numerical reflectance resulting from bulk phonon-polaritons in topological and trivial metasurfaces. Ω_R between the arrows indicates the Rabi splitting between the upper and lower polaritons for the two cases. (D) Spectral position and fraction (f_{TO}) of the phononic component in bulk polaritons. Dotted lines in (C) and (D) show the photonic bands without hBN.



in such a system at optical frequencies (22, 23). Here, we tailor this metasurface to support bulk modes in the mid-IR frequency range (near $\omega_{TO} = 1368 \text{ cm}^{-1}$, which corresponds to the wavelength $\lambda \approx 7.31 \mu\text{m}$, where ω_{TO} is the transverse optical (TO) phonon resonance frequency of hBN) (Fig. 1B) to enable their hybridization with TO phonons in hBN (24–26).

The addition of the hBN layer on top of the metasurface leads to coupling between photonic and phononic modes, giving rise to the formation of hybrid polaritonic states. The condition of strong coupling, required for the observation of topological phonon-polaritons (20), can be achieved when the hBN thickness exceeds $\sim 5 \text{ nm}$. From this point forward, we consider the case of the 15-nm-thick hBN. To confirm the strong coupling regime, we performed full-wave numerical calculations. The calculated reflectance in the vicinity of the lower bulk photonic bands and the phonon line is shown in Fig. 1C, which evidences the formation of lower and upper phonon-polaritons with a Rabi splitting (Ω_R) of $\sim 8.15 \text{ meV}$ and 8.40 meV (supplementary note 1) (27) for topological and trivial cases, respectively. We then extracted the polaritonic band structure by tracing the maxima of energy stored in the system, shown in Fig. 1D, which confirms the avoided crossing behavior. The color in Fig. 1D indicates the fraction of the phonon component in the polaritonic mode f_{TO} , which can be directly related to the Hopfield coefficient of the mode (supplementary note 2) (27). It is worth noting here that our system represents a polaritonic system, and thus, it should be differentiated from recent demonstrations of topological phases for pure mechanical modes (28–30). TO phonons in hBN are characterized by vanishing group and energy velocities at small phonon wave numbers; therefore, lattice vibrations do not directly contribute to the energy transfer of the reported polaritonic modes (supplementary note 4) (27). The transport of vibrations is thus mediated by the electromagnetic field strongly coupled to phonons through the polarization of hBN.

An important consequence of the strong coupling is the transfer of topological invariant from the photonic mode to the upper polaritonic mode (20), which is ultimately responsible for the formation of topologically robust helical edge phonon-polaritons. A calculation of the topological invariants shows that, for the case of a TO phonon crossing the lower photonic (EM) bulk mode [$\omega_{TO} < \omega_{EM}(k = 0)$], the upper polariton acquires spin-Chern numbers $C_s = \pm 1$ for the two pseudospins (supplementary note 3) (27)—a scenario realized in the experiment described below. For the case of the TO phonon line above the lower photonic bulk mode, the spin-Chern number is transferred to the lower polariton instead.

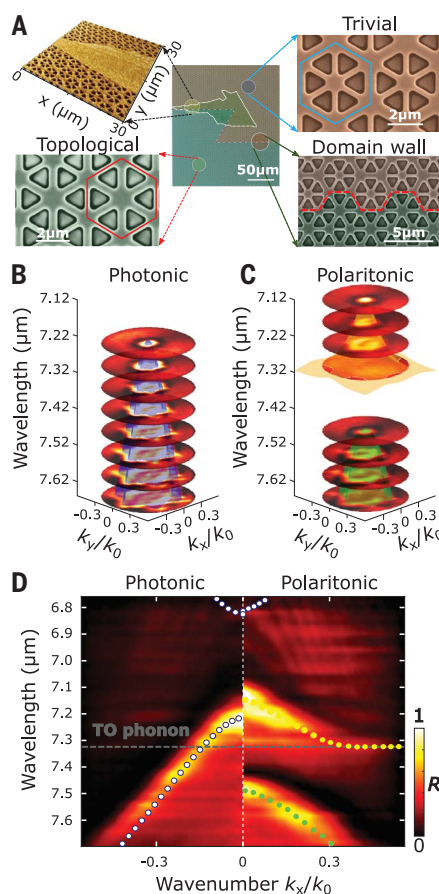


Fig. 2. Experimental evidence of topological phonon-polariton formation. (A) SEM images of metasurface with trivial (orange-shaded) and topological (green-shaded) domains separated by an armchair-shaped domain wall. Zoom-ins show enlarged regions with hBN obtained by atomic force microscopy (AFM), with topological and trivial domains, and the domain wall. (B) Raw data: Experimental constant-frequency contours imaged from the region without hBN and representing slices of lower photonic bands in Fig. 1, B and D. The blue semitransparent surface shows calculated dispersion. (C) Raw data: Experimental constant-frequency contours corresponding to the region with hBN and corresponding to the bulk polaritonic bands in Fig. 1, C and D. The semitransparent bands show calculated dispersions of lower (green) and upper (yellow) bulk phonon-polaritons. (D) Slices of a 3D Fourier tomogram showing frequency bands along the x direction. Left and right halves correspond to photonic (no hBN) and polaritonic (with hBN) cases. The dotted lines show simulated photonic (white) and polaritonic (yellow and green) band dispersions. The trivial domain case with bright dipolar bands is shown in (B) through (D). The topological domain data are provided in fig. S4.

To experimentally confirm strong coupling between photonic and phononic modes, and at the same time to enable the observation of topological edge phonon-polaritons, a sample characterized by a zigzag-shaped domain wall

was fabricated by patterning a 1- μm SOS substrate (Fig. 2A). A 15-nm hBN layer was transferred on top to cover half of the zigzag (Fig. 2A), which enabled a direct comparison of topological photonic and polaritonic regimes.

A home-built mid-IR imaging system (fig. S1) was used for both real-space and Fourier plane imaging of the sample (supplementary materials, materials and methods section) (27). This system allows the extraction of a sequence of constant frequency contours (a Fourier tomogram), with Fig. 2, B and C, illustrating the case of a trivial metasurface without and with hBN, respectively, near the polaritonic modes. In agreement with our numerical results, the addition of the 15-nm hBN layer alters the band structure as a result of the strong coupling, leading to the formation of the upper polariton, which asymptotically approaches the TO phonon line, and of the lower polariton, which asymptotically approaches the lower photonic band. The polariton formation is even more obvious from the slices of the three-dimensional (3D) band structure taken in the k_x -direction (Fig. 2D), which compares photonic and polaritonic cases side by side.

We then confirmed the presence of helical polaritonic edge states and their robustness. We collected both Fourier plane and real-space images of the structure under linear and circularly polarized illumination in the regions with and without hBN at the domain wall. As a reference, the numerically calculated reflectivity spectra from the region near the domain wall (Fig. 3A) clearly show edge states in both photonic and polaritonic regimes. Extraction of the spectral position of the edge bands for both cases is then done by tracing the stored energy maximum (Fig. 3B).

The top panel of Fig. 3C shows experimental Fourier space images along the domain walls obtained for left circularly polarized (LCP) excitations. These images reveal the one-way character and helical nature of the edge states for both photonic (left) and polaritonic (right) cases. The bottom panel shows the spectral position of the edge states extracted from the reflectivity spectra. In agreement with bulk-boundary correspondence and our theoretical predictions in Fig. 3, A and B, the edge states asymptotically approach the upper polaritonic band that carries a nonzero spin-Chern number. The excellent agreement between experimental results and the simulations in Fig. 3, A and B, implies that our numerical results can be used to explore otherwise inaccessible properties of the edge states. Specifically, we can conclude that the edge polaritons carry a substantial phononic component, which reaches 50% at $k_x = 0$. By directly calculating transverse angular momentum (fig. S3), we also deduce that the edge phonon-polaritons inherit the helical nature of the photonic modes (supplementary note 5) (27).

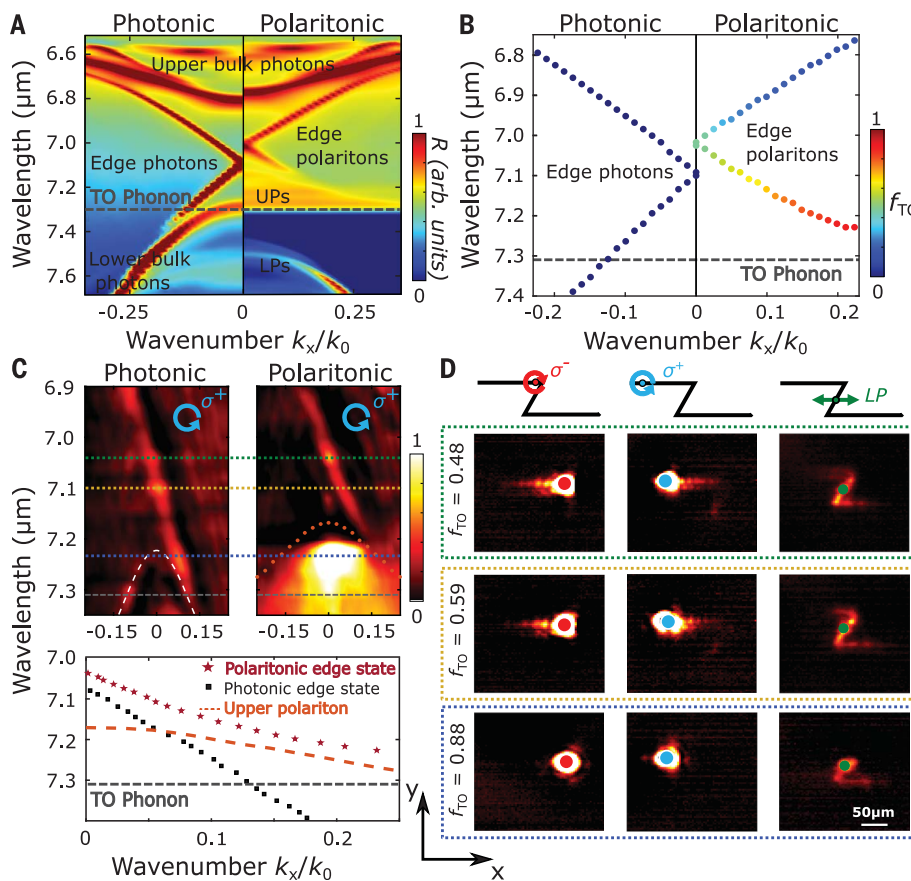


Fig. 3. Topological edge phonon-polaritons. (A) Numerical reflectivity spectra of topological domain wall revealing photonic and polaritonic edge states. UPs, upper polaritons; LPs, lower polaritons. (B) Numerically calculated spectral position and phononic fractions of the edge polaritons. (C) (Top) Experimental Fourier plane images revealing dispersion of edge states. (Bottom) Dispersion of edge states extracted from reflectivity spectra. (D) Unidirectional (left and middle panels) and bidirectional (right panels) excitation of the edge states by circularly and linearly polarized (LP) laser beam, respectively. The beam is focused on different locations of the domain wall (indicated by the top insets) for three different frequencies [color-coded dashed lines indicate the frequencies in (C)] for increasing phononic fraction f_{TO} . Cross-polarized collection suppresses the laser spot in the right panels. The gray dashed lines in (A) and (C) indicate the spectral position of the TO phonon mode. The white dashed line and brown dotted line show the calculated dispersion of bulk photonic and upper polaritonic bands, respectively.

The helical character of edge phonon-polaritons in real space and their robustness were confirmed in a series of measurements with excitation at different locations (indicated in the top inset of Fig. 3D) along the zigzag of the domain wall and for different frequencies. First, edge polaritons were excited with a circularly polarized beam, and we observed unidirectional propagation (left and middle panels in Fig. 3D) of the modes. Second, linearly polarized light was used to excite the edge state in the middle of the zigzag, exactly at the boundary of the hBN flake (Fig. 2A). This configuration allowed us to observe polaritonic and photonic edge states at once. We can see that, like the photonic edge states, the edge phonon-polaritons exhibit topological resilience concerning sharp bending, with the only difference of shorter propagation length

because of the absorption in hBN. Nonetheless, the propagation distance of the edge polaritons reaches $\sim 80 \mu\text{m}$ for $k_x = 0$ (upper row in Fig. 3D), despite the 50% phonon fraction (compared with $\sim 150 \mu\text{m}$ for the purely photonic scenario). As expected, for the frequencies below the bulk upper polariton (lower row in Fig. 3C), the edge mode is observed only in the region without hBN, again confirming that the polaritonic edge state originates from the bulk upper polariton carrying a topological charge. More details on the comparison of propagation features of the edge states can be found in fig. S5 (supplementary section 7) (27).

Our results reveal a topological polaritonic phase with resilient helical boundary states representing half-light half-phonons trapped to a topological mid-IR metasurface integrating a few-layer hBN. Our work provides an

opportunity to manipulate phonons by endowing them with topological characteristics through their hybridization with topological light. Topological phonon-polaritons pave the way for robust and unidirectional heat sinks and can lay the foundation for Raman spectroscopy with structured vibrations carrying angular momentum locked to their propagation direction.

REFERENCES AND NOTES

1. L. Lu, J. D. Joannopoulos, M. Soljačić, *Nat. Photonics* **8**, 821–829 (2014).
2. T. Ozawa et al., *Rev. Mod. Phys.* **91**, 015006 (2019).
3. Z. Yang et al., *Phys. Rev. Lett.* **114**, 114301 (2015).
4. S. D. Huber, *Nat. Phys.* **12**, 621–623 (2016).
5. B. Bahari et al., *Science* **358**, 636–640 (2017).
6. G. Harari et al., *Science* **359**, eaar4003 (2018).
7. M. A. Bandres et al., *Science* **359**, eaar4005 (2018).
8. D. Leykam, K. Y. Bliokh, C. Huang, Y. D. Chong, F. Nori, *Phys. Rev. Lett.* **118**, 040401 (2017).
9. S. Weimann et al., *Nat. Mater.* **16**, 433–438 (2017).
10. D. Smirnova, D. Leykam, Y. Chong, Y. Kivshar, *Appl. Phys. Rev.* **7**, 021306 (2020).
11. L. J. Maczewsky et al., *Science* **370**, 701–704 (2020).
12. S. Mukherjee, M. C. Rechtsman, *Science* **368**, 856–859 (2020).
13. D. N. Basov, M. M. Fogler, F. J. Garcia de Abajo, *Science* **354**, aag1992 (2016).
14. V. Peano, C. Brendel, M. Schmidt, F. Marquardt, *Phys. Rev. X* **5**, 031011 (2015).
15. T. Karzig, C. E. Bardyn, N. H. Lindner, G. Refael, *Phys. Rev. X* **5**, 031001 (2015).
16. A. V. Nalitov, D. S. Solnyshkov, G. Malpuech, *Phys. Rev. Lett.* **114**, 116401 (2015).
17. M. Milićević et al., *2D Mater.* **2**, 034012 (2015).
18. S. Klempt et al., *Nature* **562**, 552–556 (2018).
19. W. Liu et al., *Science* **370**, 600–604 (2020).
20. M. Li et al., *Nat. Commun.* **12**, 4425 (2021).
21. L. H. Wu, X. Hu, *Phys. Rev. Lett.* **114**, 223901 (2015).
22. S. Barik et al., *Science* **359**, 666–668 (2018).
23. N. Parappurath, F. Alpeggiani, L. Kuipers, E. Verhagen, *Sci. Adv.* **6**, eaaw4137 (2020).
24. S. Dai et al., *Science* **343**, 1125–1129 (2014).
25. M. Autore et al., *Light Sci. Appl.* **7**, 17172 (2018).
26. J. D. Caldwell et al., *Nat. Rev. Mater.* **4**, 552–567 (2019).
27. See the supplementary materials.
28. R. Süssstrunk, S. D. Huber, *Science* **349**, 47–50 (2015).
29. J. P. Mathew, J. del Pino, E. Verhagen, *Nat. Nanotechnol.* **15**, 198–202 (2020).
30. H. Ren et al., Topological phonon transport in an optomechanical system. arXiv:2009.06174 [cond-mat.mes-hall] (2020).
31. S. Guddala et al., Topological phonon-polariton funneling in mid-infrared metasurfaces, version 2, Zenodo (2021); <https://doi.org/10.5281/zenodo.5524881>.

ACKNOWLEDGMENTS

Funding: The work was supported by the ONR award N00014-21-1-2092, NSF grants DMR-1809915 and OMA-1936351, the DARPA Nascent program, and the Simons Collaboration on Extreme Wave Phenomena. A.A. acknowledges support by ONR award N00014-19-1-2011 and a Vannevar Bush Faculty Fellowship. **Author contributions:** A.B.K. and S.G. conceived the project. S.G., F.K., S.K., and A.V. performed the experiments. A.B.K., M.L., S.G., A.V., and S.K. performed theoretical studies. A.B.K., A.A., and V.M.M. supervised the research. A.B.K. and S.G. wrote the manuscript with input from all coauthors. **Competing interests:** The authors declare no competing interests. **Data and materials availability:** All data are deposited at Zenodo (31).

SUPPLEMENTARY MATERIALS

science.org/doi/10.1126/science.abj5488
Materials and Methods
Supplementary Text
Figs. S1 to S8
References (32–39)

19 May 2021; accepted 31 August 2021
[10.1126/science.abj5488](https://science.org/doi/10.1126/science.abj5488)

Topological phonon-polariton funneling in midinfrared metasurfaces

S. Guddala¹ F. Komissarenko² S. Kiriushchikina³ A. Vakulenko⁴ M. Li⁵ V. M. Menon⁶ A. Alù⁷ A. B. Khanikaev⁸

Science, 374 (6564), • DOI: 10.1126/science.abj5488

Coupling light and heat

Understanding of the topological features of bandgaps has provided a route for engineering optical structures that exhibit directional propagation of light and are robust to defects. Guddala *et al.* combined a silicon-based topological photonic crystal with an atomic monolayer of hexagonal boron nitride (hBN). The topological features of the photonic crystal are coupled to the lattice vibrations of the hBN through the formation of phonon-polaritons. Funneling of helical infrared phonons along arbitrary pathways and across sharp bends provides the possibility of realizing directional heat dissipation along topologically resilient heat sinks. —ISO

View the article online

<https://www.science.org/doi/10.1126/science.abj5488>

Permissions

<https://www.science.org/help/reprints-and-permissions>